

Use of integrated profiling techniques for studying cloud-radiation interactions

Kerstin Ebell¹, Susanne Crewell², Ulrich Löhnert³, and Ewan J. O'Connor⁴

¹*Institute for Geophysics and Meteorology, University of Cologne, Kerpener Str. 13, 50937 Cologne (Germany), kebell@meteo.uni-koeln.de*

²*Institute for Geophysics and Meteorology, University of Cologne, Kerpener Str. 13, 50937 Cologne (Germany), crewell@meteo.uni-koeln.de*

³*Institute for Geophysics and Meteorology, University of Cologne, Kerpener Str. 13, 50937 Cologne (Germany), loehnert@meteo.uni-koeln.de*

⁴*Department of Meteorology, University of Reading, PO Box 243, Earley Gate, Reading RG6 6BB (United Kingdom), E.J.OConnor@reading.ac.uk*

ABSTRACT

The accurate knowledge of the atmospheric state, i.e. temperature, humidity, cloud liquid water and cloud ice profiles is needed for a number of applications - the calculation of radiative flux profiles being a particularly demanding one. In order to study cloud-radiation interactions the atmospheric state has been derived for a nine month period of the Atmospheric Radiation Measurement (ARM) programs mobile facility in the Black Forest, Germany, using the Integrated Profiling Technique and the Cloudnet retrieval algorithms. The derived profiles are subsequently used as input data for radiative transfer calculations to estimate the cloud radiative effect and forcing.

1. INTRODUCTION

The spatial and temporal inhomogeneity of the incoming solar radiation is the driving mechanism for the whole weather system. To understand the variability in the surface radiation budget, it is necessary to obtain concurrent measurements of atmospheric state parameters that affect this budget. The temporal and spatial distribution of clouds is of particular interest because clouds are the most significant modulator for the surface radiation budget and the vertical distribution of energy in the atmosphere. To assess the cloud radiative effects, a data set is needed which describes the atmospheric state as accurately as possible. In this respect, the synergy of different active and passive remote sensing instruments for various wavelengths offers a unique opportunity, since the strengths of the individual measurement systems are combined.

In particular, the Integrated Profiling Technique (IPT; [1],[2]) has been successfully used to derive profiles of temperature, humidity and liquid water content (LWC) and corresponding error estimates. The IPT uses a combination of ground-based microwave radiometer (MWR) and cloud radar measurements and a priori information in the framework of the optimal estimation equations [3]. This method has been applied to

the measurements of the ARM Mobile Facility (AMF), which has been deployed in the Black Forest, Germany, between April and December 2007. The measurements by the AMF were complemented by the University of Cologne's multispectral microwave radiometers HATPRO and DPR.

Given the IPT profiles, radiative transfer calculations are performed to assess the cloud radiative effect and forcing. Two radiative transfer schemes are applied. The first one is the radiative transfer scheme of the numerical weather prediction model COSMO of the Deutscher Wetterdienst [4]. The second one is the rapid radiative transfer model RRTMG by the Atmospheric and Environmental Research, Inc., which is implemented in the ECMWF Integrated Forecast System. First, we present the retrieval technique and the resulting cloud profiles, followed by first results of the radiative transfer calculations.

2. INTEGRATED PROFILING TECHNIQUE

In the setup used here, the IPT employs microwave radiometer brightness temperatures at frequencies in the K-band (22-32 GHz) and in the V-band (51-59 GHz) at 7 frequencies per band from the HATPRO instrument. Additionally, measurements at 90 and 150 GHz from the DPR are used. In cloudy situations, cloud radar reflectivities are also included in the retrieval to derive LWC. Since the retrieval of temperature, humidity and LWC profiles from these measurements is an ill-conditioned problem, i.e. many solutions fit the measurements, the solution can be further constrained by a priori information. For the temperature and humidity profiles, temporally interpolated radiosonde data are used, while the LWC a priori profile is derived by a modified adiabatic model according to the authors in [5].

The atmospheric profiles and the measurements are related by a forward model which is a microwave radiative transfer operator for nonscattering cases for the brightness temperatures and a Z-LWC relationship for the radar reflectivities. Errors of measurements, forward

model and a priori profile are properly described by covariance matrices. Given these errors, the measurements and a priori information are integrated in an iterative procedure employing the optimal estimation equations (for more details see [1], [2]). Information on the occurrence and vertical location of clouds is included in the retrieval by means of the Cloudnet Target Categorization product [6], which is itself a synergy product of cloud radar, ceilometer, microwave radiometer and model data. The LWC profiles are retrieved on the cloud radar grid with a vertical resolution of about 42 m. The temperature and humidity profiles are defined on a coarser grid with a 50 m resolution for the lowest 250 m and a gradually decreasing resolution up to a height of 30 km.

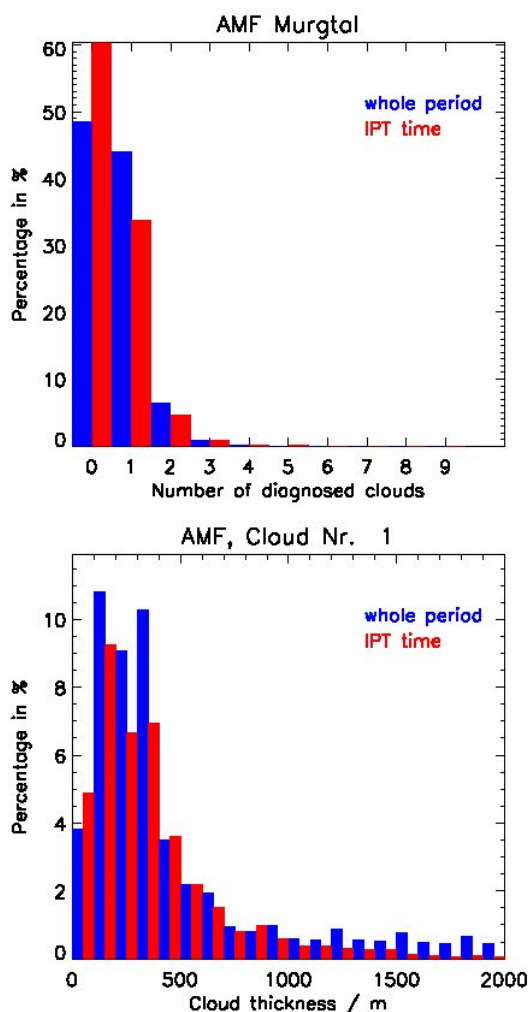


Figure 1. Water cloud statistics for the AMF Black Forest site. Number of cloud layers (top) and thickness of lowest cloud (bottom) derived from the CloudNet Target Categorization product. The blue bars show the results for the whole nine month, the red bars the results for those times the IPT converged.

3. CLOUD STATISTICS

For the nine-month measurement period, 88,110 profiles have been derived by the IPT including 33,168 scenes with water clouds. The temporal resolution of the retrieved data set is about 90 s. Data gaps are mainly due to mismatching instrument times, precipitation and melting layers. In case of rain, brightness temperatures are contaminated by the wet radome of the MWR. In melting layer situations, it is not clear which fraction of the radar signal can be attributed to the liquid phase. Thus, the retrieval of the profiles is not possible in these cases.

Figure 1 shows some water cloud statistics derived from the Cloudnet Categorization data. About 42% of all profiles contain single layer water clouds which have a cloud thickness of 100-400 m. Because of the previously mentioned restrictions on the application of the IPT, the statistics for the IPT times are slightly different. Since certain cloudy cases are excluded, we have relatively more cloud-free cases.

The distribution of the LWC of the 33,168 cloudy profiles together with the mean LWC profile is shown in Figure 2. LWC values mostly range between 0.025 and 0.15 gm^{-3} and are located in a height of 200 to 2000 m. Larger LWC values up to 0.6 gm^{-3} can be mainly found between 500 and 1000 m, which is also reflected in the mean LWC profile.

4. RADIATIVE TRANSFER CALCULATIONS

The IPT profiles can be used to assess the cloud radiative effect (CRE) and forcing (CRF) of these clouds. For this purpose, we use two different radiative transfer schemes, i.e the radiation scheme by the authors in [4] and the rapid radiative transfer model RRTMG [7].

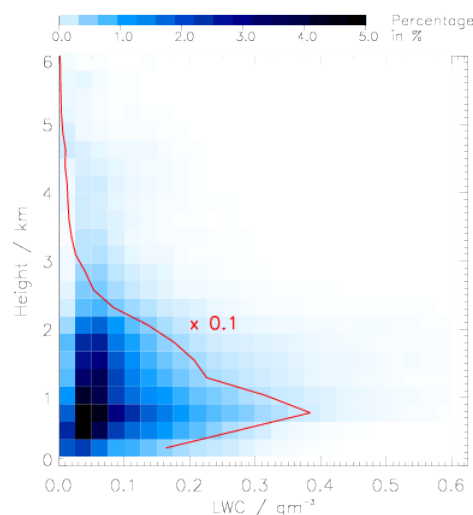


Figure 2. Frequency distribution of LWC with height. The red line indicates the mean LWC profile of all cloudy profiles. Note that the values of the mean profile have been multiplied by 10 to fit the x-axis.

The first one is implemented in the numerical weather prediction model COSMO of the Deutscher Wetterdienst. It is based on the δ -two-stream approximation of the radiative transfer equation, which is solved for 3 solar and 5 thermal spectral intervals. The RRTMG has been developed by the Atmospheric Environmental Research, Inc. Fluxes and heating rates are calculated over 14 contiguous bands in the shortwave and 16 in the longwave regime. For multiple scattering, a two-stream algorithm after is used [8]. In the RRTMG, the optical properties of water clouds are calculated for each spectral band according to the parameterization of the authors in [9]. The droplet effective radius is also needed as an input parameter in the RRTMG, while in the COSMO scheme, it is parameterized in terms of the cloud liquid water. For the RRTMG, the droplet effective radius is calculated according to method in [10] with an assumed total number concentration of 288 cm^{-3} and a lognormal size distribution width of 0.38 [11]. As an example, the derived LWC profiles for a stratocumulus cloud layer on 8 September, 2007, are shown in Figure 3. The corresponding shortwave, longwave and net CRF can be seen in Figure 4. The vertical resolution of radiative transfer calculations is 50 m in the lowest 250 m and decreases with height, e.g. 250 m at 2 km and 500 m at 5 km.

Shortwave warming is strong at cloud top (up to 20 K day^{-1}). Below the cloud layer, a weak cooling (about -2 K day^{-1}) takes place. Longwave cooling is pronounced at cloud top showing values of about -40 to -50 K day^{-1} . Below the cloud, the atmosphere is warmed in the longwave region. In levels adjacent to cloud base, warming is up to 16 K day^{-1} , while in the layers below, the CRF is approximately 2 K day^{-1} . During daytime, the warming in the lowest levels is mostly compensated by shortwave cooling, leading to a net CRF of about 0.2 - 0.4 K day^{-1} in these heights. At cloud top, the net CRF is dominated by longwave cooling, although SW warming slightly reduces the energy loss during daytime.

The results of both models are quite similar. However, the radiation scheme of the COSMO model shows a tendency to a stronger cooling at the top of the cloud (about 10 K day^{-1}) and a stronger warming of about 3 K day^{-1} in the layers directly below the cloud. These differences have to be investigated in more detail, since they may also be a result of different computations of

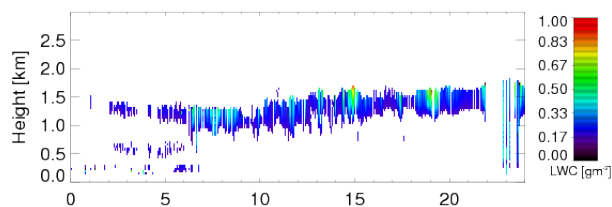


Figure 3. LWC profiles on 8 September 2007 (gm^{-3}).

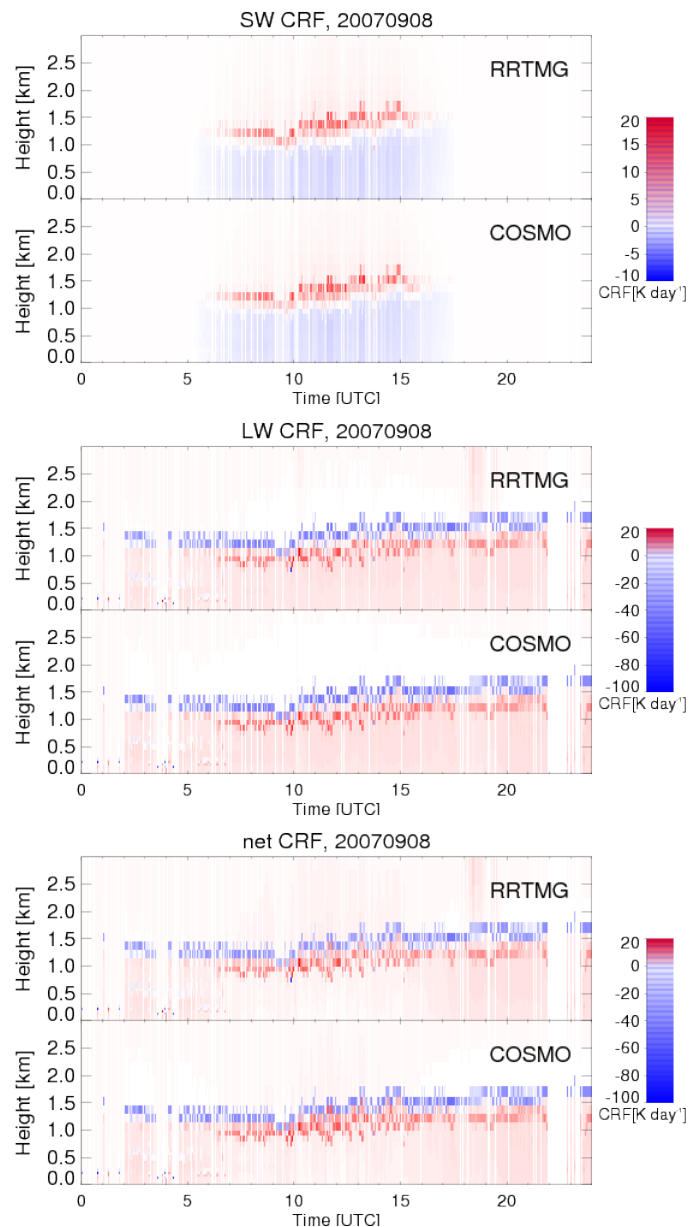


Figure 4. Shortwave (top), longwave (middle), and net CRF (bottom) in K day^{-1} . The results for both radiative transfer models, COSMO and RRTMG, are shown.

the droplet effective radius in both models.

5. OUTLOOK

We will extend the analysis of the cloud statistics and evaluate the retrieved profiles via radiative closure studies. Differences between observed and modelled fluxes may also be related to horizontal inhomogeneities of the cloud fields, which are not included in the radiative transfer calculations. In this respect, the measurements of our azimuth-scanning MWR HATPRO can be

included in the analysis, since these measurements give a hint on the horizontal variability of the integrated waver vapor and the liquid water path.

The radiative effect of clouds will be assessed for the whole measurement period in the Black Forest including also ice clouds. For this purpose, the ice water content (IWC) from the Cloudnet retrieval algorithms will be used. Uncertainties in the radiative fluxes and heating rates due to uncertainties in the LWC and IWC profiles will be assessed, as well as uncertainties due to different radiative transfer parameterizations.

ACKNOWLEDGMENTS

For the IPT, data were obtained from the Atmospheric Radiation Measurement (ARM) Program sponsored by the U.S. Department of Energy, Office of Science, Office of Biological and Environmental Research, Climate and Environmental Sciences Division. We would like to thank Wenchieh Yen who helped with the implementation of the radiative transfer model RRTMG.

REFERENCES

- [1] Löhnert, U., S. Crewell, C. Simmer, 2004: An integrated approach towards retrieving physically consistent profiles of temperature, humidity and cloud liquid water, *Journal of Applied Meteorology*, 43 (9), pp. 1295-1307.
- [2] Löhnert, U., S. Crewell, O. Krasnov, E. O'Connor, H. Russchenberg, 2008: Advances in continuously profiling the thermodynamic state of the boundary layer: integration of measurements and methods, *Journal of Atmospheric and Oceanic Technology*, 25, pp. 1251-1266.
- [3] Rodgers C. D., 2000: *Inverse methods for atmospheric sounding: theory and practice*, World Scientific, 238 pp.
- [4] Ritter, B., J.-F. Geleyn, 1992: A comprehensive radiation scheme for numerical weather prediction models with potential applications in climate simulations, *Monthly Weather Review*, 120, pp. 303-325.
- [5] Karstens, U., C. Simmer, E. Ruprecht, 1994: Remote sensing of cloud liquid water, *Meteorology and Atmospheric Physics*, 54, pp. 157-171.
- [6] Illingworth, A. J., R. J. Hogan, E. J. O'Connor, D. Bounoil, M. E. Brooks, J. Delanoë, P. Donovan, J. D. Eastment, N. Gaussiat, J. W. F. Goddard, M. Haefelin, H. Klein, H. Klein Baltink, O. A. Krasnov, J. Pelon, J.-M. Piriou, A. Protat, H. W. J. Russchenberg, A. Seifert, A. M. Tompkins, G.-J. van Zadelhoff, F. Vinit, U. Willén, D. R. Wilson, C. L. Wrenchand, 2007: CLOUDNET Continuous evaluation of cloud profiles in seven operational models using ground-based observations, *Bulletin of the American Meteorological Society*, 88 (6), pp. 883-898.
- [7] Clough, S.A., M.W. Shephard, E.J. Mlawer, J.S. Delamere, M.J. Iacono, K. Cady-Pereira, S. Boukabara, P.D. Brown, 2005: Atmospheric radiative transfer modeling: a summary of the AER codes, *Journal of Quantitative Spectroscopy and Radiative Transfer*, 91, pp. 233-244.
- [8] Oreopoulos, L., H.W. Barker, 1999: Accounting for subgrid-scale cloud variability in a multi-layer 1-D solar radiative transfer algorithm, *Quart. J. Roy. Meteor. Soc.*, 125, pp. 301-330.
- [9] Hu, Y.X., K. Stamnes, 1993: An accurate parameterization of the radiative properties of water clouds suitable for use in climate models, *Journal of Climate*, 6, pp. 748-742.
- [10] Frisch, A.S., C.W. Fairall, J.B. Snider, 1995: Measurement of stratus cloud and drizzle parameters in ASTEX with a K_{α} -Band doppler radar and a microwave radiometer, *Journal of the Atmospheric Sciences*, 52, pp. 2788-2799.
- [11] Miles, N.L., J. Verlinde, E.E. Clothiaux, 2000: Cloud droplet size distributions in low-level stratiform clouds, *Journal of the Atmospheric Sciences*, 57, pp. 295-311.